Superlattices and Microstructures, Vol. 20, No. 3, 1996

Nano-particle transistors and energy-level spectroscopy in metals

D. C. RALPH†, C. T. BLACK‡, M. TINKHAM
Department of Physics and Division of Applied Sciences, Harvard University, Cambridge, Massachusetts 02138, U.S.A.

(Received 20 May 1996)

We report the fabrication of single-electron tunneling transistors consisting of a single nm-scale aluminum particle connected via tunnel junctions to two leads and capacitively coupled to a third gate electrode. We have used these devices to measure the spectra of discrete electronic quantum energy levels in the particle while tuning the number of electrons it contains.

Key words: energy levels, single-electron tunneling, transistor.

In recent years there has been rapid development of several techniques for fabricating tunneling devices made from nanometer-scale particles [1–5]. This work is motivated by at least two main goals. The first is the eventual production of single-electron tunneling devices [6] which operate at high temperatures, much higher than the 1 K scale achieved by devices made using conventional electron beam lithography. Several of the articles in these proceedings report progress along this path. In this paper we will concentrate primarily on a second, very different, subject. Metal particles less than about 10 nm in diameter are small enough that the energy spacing between their discrete 'electrons-in-a-box' energy levels is larger than thermal energies $k_B T$ for temperatures below 1 K. These energy levels can be measured using tunnel junction devices incorporating a single nm-scale metal particle, because electrons can traverse the device only by tunneling via the discrete states in the particle. At low temperature, the current–voltage (I–V) curve consists of a sequence of small steps, from which the spectrum of excited states can be read directly. This new ability to measure the spectrum of electronic energy levels within a metal sample is valuable from a basic science viewpoint, because this spectrum gives detailed microscopic information about all the forces which shape electronic structure in the metal. One may bring to solid state physics many of the habits of thought of atomic physicists, learning about the physics which controls electronic properties by studying the behavior of electronic energy levels. Nanometer-scale metal particles may be considered 'artificial atoms' in the same way as micron scale quantum dots formed from semiconductor two-dimensional electron gases [7].

We have previously described measurements on devices which consisted of a single nm-scale Al particle connected to two separate macroscopic leads by high-resistance tunnel junctions [8–10]. These studies revealed

† Present address: Physics Department, Cornell University, Ithaca, NY 14853, U.S.A.

‡ Present address: IBM T. J. Watson Research Center, Yorktown Heights, NY 10598, U.S.A.

0749–6036/96/070389 + 06 $18.00/0

how examination of electronic energy level spectra in metals provides new information about superconducting pairing forces, electron–electron interactions, spin–orbit scattering, and effects of the electron-number parity in a metal particle. Here we will report initial results from a new generation of devices—nano-particle transistors—made by adding a third (gate) electrode in close proximity to the nm-scale particle. The gate electrode allows greatly increased flexibility in the study of electronic spectra, for instance by allowing us to tune controllably the number of electrons in the ground state of the particle. An expanded, more detailed article about our measurements is in preparation.

Figure 1 depicts a cross-sectional schematic of our device geometry. Sample fabrication begins with a suspended membrane of low-stress Si_3N_4, 50 nm thick. Following the procedure of Ralls *et al*. [11], we use electron-beam lithography and reactive ion etching to form a bowl-shaped hole through the membrane, with an opening at the lower edge of the membrane roughly 5–10 nm in diameter. We then deposit 12 nm of Al through a stencil mask onto the flat side of the membrane (the bottom part of Fig. 1) to form the gate electrode. The difficult part of the process is to achieve electrical isolation between this gate and the other metal layers which are to follow, without plugging the nm-scale hole. We do this by plasma anodization of the Al film, to a bias of 3 V, followed by deposition of 6 nm of SiO onto liquid-nitrogen cooled samples. This procedure produces pinhole-free barriers without clogging the nm-scale hole in 80–90% of devices. The rest of the fabrication process is similar to that used in our previous samples [8–10]. We deposit a thick film of Al (100nm) onto the bowl-shaped side of the membrane. As Al fills the bowl, the grains grow together and coalesce to form an interface in the vicinity of the lower edge of the membrane. We then oxidize for 45 s in 7 Pa of O_2 at room temperature, to form a tunnel barrier at this interface. A layer of nm-scale Al particles is formed by evaporating a (discontinuous) film of Al (3 nm by mass) onto the flat side of the membrane. We rely on luck to have one nm-scale particle form in contact with the tunnel junction in the nano-hole. (After the completion of device fabrication, we can quickly pick out these good devices by looking for Coulomb staircase I–V curves at 4.2 K, and we achieve a yield of about 25%.) We then produce a second tunnel barrier on the exposed surface of the particle with a second oxidation step, and finally deposit a thick Al electrode over the layer of particles by evaporation through a stencil mask. We measure I–V curves for electrons tunneling from one Al lead through the nano-particle to the second lead, while adjusting the electrostatic potential of the particle with the gate electrode.

In Fig. 2 we plot the evolution of the large-scale Coulomb-staircase I–V curve as a function of gate voltage for two of our samples at 4.2 K. Both show large regions of Coulomb blockade near zero bias, with current ramps and evenly spaced steps at higher bias that are characteristic of single-electron tunneling via an individual nm-scale metal particle [12]. The effect of the applied gate voltage is to adjust the energy imbalance between states with different numbers of electrons on the metal particle, thus tuning the size of the Coulomb blockade region. Each time the blockade region is tuned through zero, the number of electrons in the ground state of the particle is changed by one. From the voltage thresholds for the ramps and steps composing the Coulomb staircase curve, we can determine the capacitances of the tunnel junctions within the device [12]. For the sample of Fig. 2A, the lead-to-particle capacitances are 3.5 and 9.4 aF, and the gate-to-particle capacitance is 0.1 aF, giving a Coulomb-blockade energy $E_c = e^2/(2C_{\text{total}}) = 6.1$ meV. The device in Fig. 2B has the largest E_c of our samples to date; the lead-to-particle capacitances are 0.6 and 1.0 aF, the gate-to- particle capacitance is 0.13 aF, and $E_c = 46$ meV. The gate-to-lead leakage resistance at low temperature is $10^{10}\Omega$ for the sample of Fig. 2A and was not measured for Fig. 2B.

A rough estimate may be made for the size of the nanoparticle within each device based on the larger lead-to-particle capacitance. The capacitance per unit area of the oxide tunnel junctions made using our process is approximately 0.075 aF nm^{-2}. If we make the crude assumption that the particles are roughly hemispherical, the measured capacitances imply a particle radius of 4.5 nm for the device of Fig. 2A and 1.5 nm for Fig. 2B.

We have made extensive investigations of the discrete 'electrons-in-a-box' energy levels inside the nanoparticle for the sample in Fig. 2A. The discrete levels are best observed by using the gate to tune the Coulomb tunneling threshold to low voltage, to minimize non-equilibrium and heating effects. We then make transport

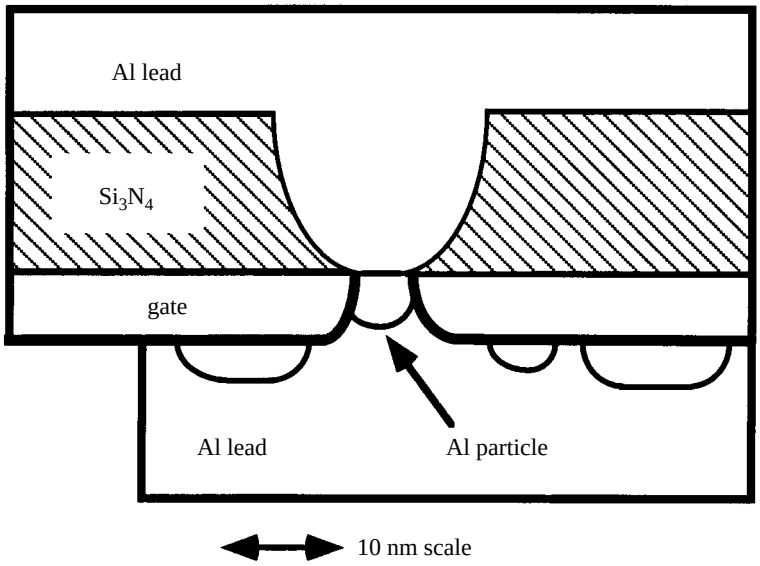

Fig. 1. Cross-sectional schematic of a nano-particle transistor.

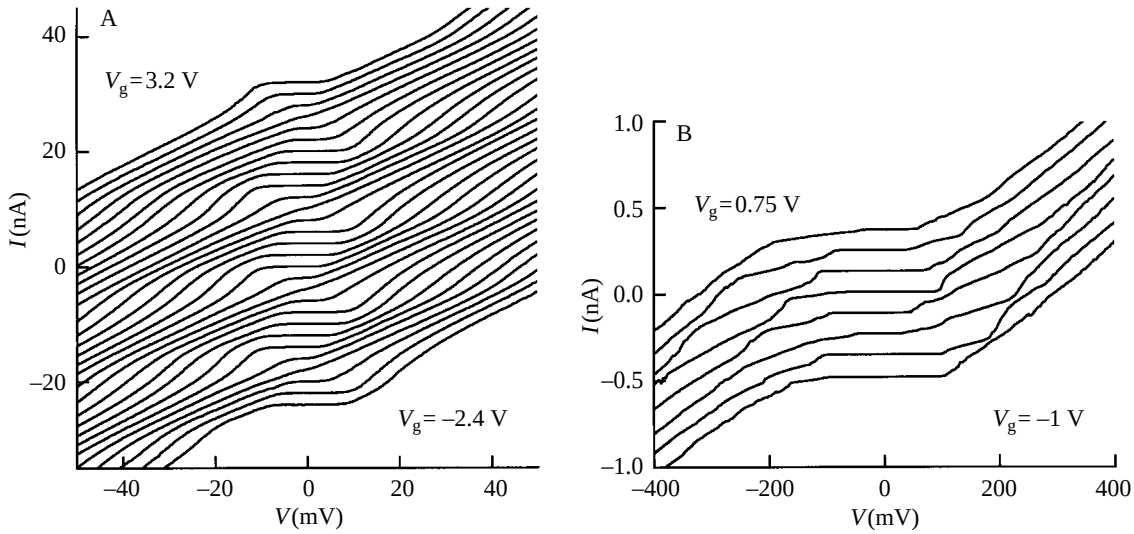

Fig. 2. Coulomb-staircase I–V curve at 4.2 K for two devices, at equally spaced increments of gate voltage. The curves are artificially offset on the current axis.

measurements at 50 mK along the initial ramp of the Coulomb-staircase curve. Because of the tunneling via discrete electronic states on the particle, the onset of current flow within the Coulomb staircase curve is not a smooth function, but consists of a fine structure of small steps in the I–V curve, or peaks in $\mathrm{d}I/\mathrm{d}V$ (Fig. 3). (The current in the Coulomb staircase curve is due to tunneling via discrete energy levels within the Al particle.) All the peaks in Fig. 3 are repeatable over time. They are all on the same initial ramp of the staircase curve, at voltages less than the threshold required to change the charge state of the Al particle

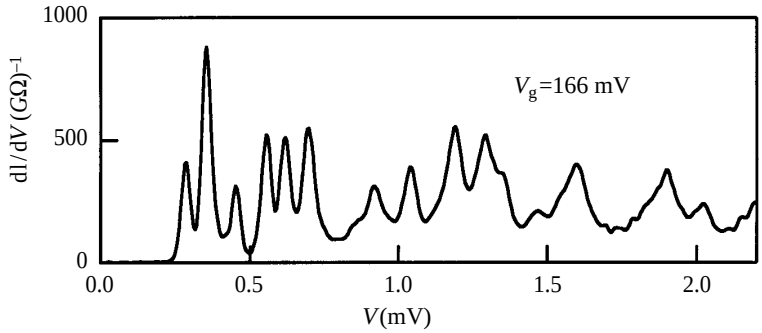

Fig. 3. Differential conductance versus voltage, in the range of the first Coulomb staircase ramp, for the device of Fig. 2A. $H = 0.05$ T (in order to drive the Al leads normal) and $T = 50$ mK.

by more than a single electron. The peaks are shifted to higher voltage, all at the same rate, by increases in the gate voltage. These observations imply, first, that all the energy levels contributing to this spectrum are due to states on the same particle, because quantum states on other particles with different capacitance values would shift at different rates with changing gate voltage. Also, all the states shown in Fig. 3 correspond to the same number of electrons on the particle—one less than the number in the ground state for $V_g = 166$ mV. (We can tell that the number of electrons on the particle *decreases* by one in the tunneling transitions because the threshold voltages *increase* with increasing gate voltage.) The different energy levels do not correspond to different charge states; they simply provide alternative channels for sequential single-electron tunneling. The measured widths of the peaks are broad enough that not all the energy levels contributing to transport are necessarily resolved, especially at higher voltages.

In Fig. 4A we display the magnetic field (H) dependence of all the resolvable peaks in the spectrum of Fig. 3 (measured at slightly higher gate voltage than in Fig. 3 so that none of the peaks cross $V = 0$ as H is varied). The voltage positions of the peaks have been converted to an energy scale by multiplying by the appropriate capacitance ratio $C_1/(C_1 + C_2) = 0.73$ [8]. All the peaks in this spectrum display Zeeman spin splitting as a function of field, with g-factors between 1.95 and 2.0. The fact that the lowest-energy tunneling transition displays Zeeman splitting, in particular, indicates that both spin states of the lowest unoccupied orbital eigenstate are empty and available for tunneling when the particle is in its ground state. This means that the tunneling transitions in these diagrams correspond to a change from an even to an odd number of electrons in the particle [8]. (For a particle with an odd number of electrons in its ground state, the lower-energy spin state for this orbital level would be occupied and unavailable for tunneling—see below.) The upward-moving spin states can be followed for only a limited range of field before they become indistinguishable from the background. There are likely several contributing factors why these upward- moving states are more difficult to resolve than the downward- moving spin states. Upward-moving states have higher excitation energies, and may therefore have greater lifetime broadening than downward-moving states, making resolution more difficult. The higher-energy states may also be masked by increased heating effects. Finally, as the voltage and current flow is increased, the particle spends a greater percentage of time in its excited charge state (with one fewer electron than in the ground state), which blocks further single-electron tunneling until the original charge number is restored. This duty-cycle effect can reduce the relative amplitude of signals due to higher-lying energy levels.

As a function of magnetic field, the energy of the first tunneling transition in Fig. 4A decreases steadily until about 4 Tesla, where it begins undergoing a zig-zag motion. The zig-zagging is due to the crossing of downward moving unoccupied energy levels with upward moving occupied levels. At each crossing, the ground state of the electrons in the particle is changed. The energy threshold for tunneling at low magnetic

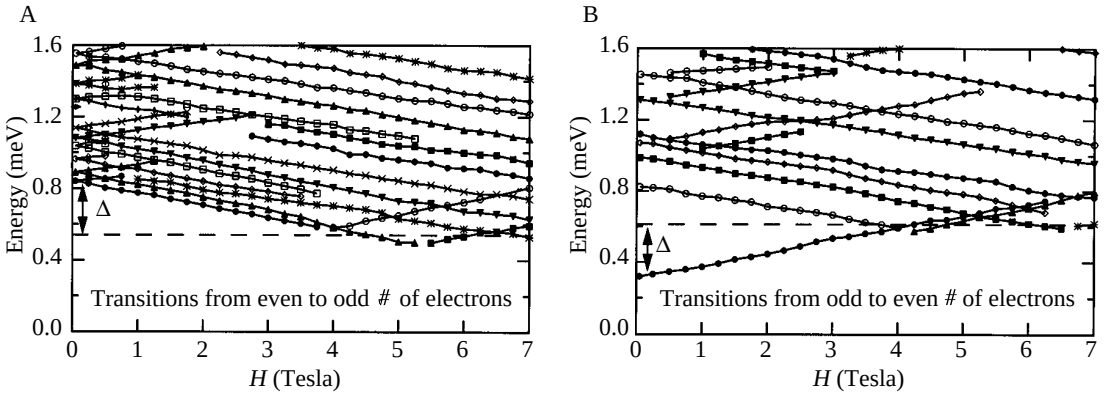

Fig. 4. Magnetic-field dependence of the resolved tunneling transitions for the gate voltage values (A) $V_g = 181$ mV and (B) $V_g = 110$ mV, for the same device as Figs. 2A and 3.

field is significantly greater than the threshold beyond 4 T, by an amount much larger than the average spacing between energy levels. The extra gap at low field illustrates the presence of superconductivity in the nm-scale Al particle [9]. At low H, the electronic ground state of the even-electron superconducting particle is fully Cooper-paired. Any transition in which an electron tunnels off the particle must leave an unpaired quasiparticle on the Al grain, so that tunneling requires an extra energy Δ, relative to the case at large magnetic field where superconductivity is suppressed. We can measure the extra tunneling gap, Δ, present when the particle is in the superconducting state, as the energy difference between the threshold for tunneling at low field and the average threshold for fields greater than 4 T; we find $\Delta = 0.30$ meV, in line with our previous results [9]. The critical field of roughly 4 T and the magnetic-field dependence of the first tunneling transition are well explained by a combination of spin and orbital pair-breaking [9].

In Fig. 4B we show the fan diagram for the tunneling transitions which are resolvable with a gate voltage of 110 mV, for which the ground state of the particle has one fewer electron than for the ground state in Fig. 4A. The transitions shown in Fig. 4B are in an opposite sense to those in Fig. 4A, in that Fig. 4B corresponds to the addition of one electron to the particle, changing the number of electrons from odd to even. For the lowest-energy odd-to-even transition no Zeeman spin splitting is present—tunneling occurs only via a single upward-moving spin level. In an independent-electron picture, this can be understood because the lower-energy spin state for this orbital level is occupied by the odd electron in the particle's ground state, blocking the tunneling of other electrons via this state [8]. The parity of the number of electrons on the particle also has consequences for the influence of superconductivity on the energy levels. The lowest energy odd-to-even tunneling transition corresponds to the addition of an electron to form a superconducting state in which all electrons are paired. All other tunneling states must contain at least two unpaired quasiparticles, so that one may expect a large enough difference, approximately 2Δ, between the first transition energy and all others [9]. We actually find that the magnitude of this energy difference in Fig. 4B is 0.50 meV, slightly smaller than twice the gap measured in Fig. 4A. This disagreement is likely the result of a non-equilibrium suppression of superconducting gap in the Al particle when it contains two excited quasiparticles. The energy widths of the more highly excited states in the odd-to-even transitions are larger than for even-to-odd transitions, so that we are able to resolve fewer high-lying states for Fig. 4B then for Fig. 4A.

In summary, we have presented initial measurements made on single-electron tunneling transistors fabricated from individual nm-scale Al particles. Devices have been made with Coulomb-blockade energies ranging up to 46 meV. We have used the transistors to measure the spectra of discrete 'electrons-in-a-box' energy levels in the Al particles, while using the gate to tune the number of electrons present in the ground

state of the particle. The energy level spectra show dramatic effects due to the parity of the number of electrons on the particle and due to superconducting pairing interactions.

Acknowledgements—This research was supported by NSF Grant No.DMR-92-07956, ONR Grant No. N00014-96-1-0108, JSEP Grant No. N00014- 89-J-1023, and ONR AASERT Grant No. N00014-94-1-0808, and was performed in part at the Cornell Nanofabrication Facility, funded by the NSF (Grant No. ECS-8619049), Cornell University, and industrial affiliates.

References

[1] R. Wilkens, E. Ben-Jacob and R. C. Jacklevic, Phys. Rev. B **42**, 8698 (1990).
[2] C. Schonenberger, H. van Houten and H. C. Dondersloot. Europhys. Lett. **20**, 249 (1992).
[3] Y. Takahashi *et al*. Electron. Lett. **31**, 136 (1995).
[4] E. S. Snow and P. M. Campbell, Science **270**, 1639 (1995).
[5] D. L. Klein, P. L. McEuen, J. E. Bowen Katari, R. Roth and A. P. Alivisatos, Appl. Phys. Lett. **68**, 2574 (1996).
[6] For a review of Coulomb-blockade physics and single-electron tunneling devices, see D. V. Averin and K. K. Likharev, in *Mesoscopic Phenomena in Solids*, Edited by B. Altshuler, P. A. Lee and R. A. Webb, Elsevier, Amsterdam, p. 173 (1991).
[7] M. A. Kastner, Physics Today **46**, No. 1, 24 (1993).
[8] D. C. Ralph, C. T. Black and M. Tinkham, Phys. Rev. Lett. **74**, 3241 (1995).
[9] C. T. Black, D. C. Ralph and M. Tinkham, Phys. Rev. Lett. **76**, 688 (1996).
[10] D. C. Ralph, C. T. Black and M. Tinkham, Physica B **218**, 258 (1996).
[11] K. S. Ralls, R. A. Buhrman and R. C. Tiberio, Appl. Phys. Lett. **55**, 2459 (1989).
[12] A. E. Hanna and M. Tinkham, Phys. Rev. B **44**, 5919 (1991).